Transfection Mediated by Gemini Surfactants: Engineered Escape from the Endosomal Compartment

Paul C. Bell,[†,⊥] Mark Bergsma,[†] Igor P. Dolbnya,[‡] Wim Bras,[‡] Marc C. A. Stuart,[§]
Alan E. Rowan,[∥] Martinus C. Feiters,*[,∥] and Jan B. F. N. Engberts*[,†]

*Contribution from the Physical Organic Chemistry Unit, Stratingh Institute,
University of Groningen, 4 Nijenborgh, 9747 AG Groningen, The Netherlands,
DUBBLE CRG/ESRF, Netherlands Organization for Scientific Research (NWO),
c/o ESRF BP 220, F-38043 Grenoble Cedex, France, Biophysical Chemistry,
Groningen Biomolecular Sciences and Biotechnology Institute, University of Groningen,
4 Nijenborgh, 9747 AG Groningen, The Netherlands, and Department of Organic Chemistry,
University of Nijmegen, 1 Toernooiveld, 6525 ED Nijmegen, The Netherlands*

Received May 20, 2002 ; E-mail: mcf@sci.kun.nl; j.b.f.n.engberts@chem.rug.nl

Abstract: The structure of the lipoplex formed from DNA and the sugar-based cationic gemini surfactant **1**, which exhibits excellent transfection efficiency, has been investigated in the pH range 8.8−3.0 utilizing small-angle X-ray scattering (SAXS) and cryo-electron microscopy (cryo-TEM). Uniquely, three well-defined morphologies of the lipoplex were observed upon gradual acidification: a lamellar phase, a condensed lamellar phase, and an inverted hexagonal (H_{II}) columnar phase. Using molecular modeling, we link the observed lipoplex morphologies and physical behavior to specific structural features in the individual surfactant, illuminating key factors in future surfactant design, viz., a spacer of six methylene groups, the presence of two nitrogens that can be protonated in the physiological pH range, two unsaturated alkyl tails, and hydrophilic sugar headgroups. Assuming that the mechanism of transfection by synthetic cationic surfactants involves endocytosis, we contend that the efficacy of gemini surfactant **1** as a gene delivery vehicle can be explained by the unprecedented observation of a *pH-induced* formation of the inverted hexagonal phase of the lipoplex in the endosomal pH range. This change in morphology leads to destabilization of the endosome through fusion of the lipoplex with the endosomal wall, resulting in release of DNA into the cytoplasm.

Introduction

Gene therapy is an approach to treat acquired and inherited diseases by transfection, that is, ferrying a correct copy of the defective gene into the cell.[1] Viruses are the most effective transfection agents,[2] but their application is not without risk for patients.[3,4] Synthetic cationic surfactants are also effective in transfection[5,6] and are involved in 18% of current clinical trials based on gene therapy.[7] In view of the dangers of viral transfection vectors, the concept of transfection by synthetic cationic surfactants is attractive, provided that they can be further developed to compete with viral vectors in efficiency.[8]

Gemini surfactants[9] are a relatively new class of amphiphilic molecules containing two headgroups and two aliphatic chains, linked by a rigid[10,11] or flexible[12,13] spacer. They have physicochemical properties that are different from those of conventional (single chain, single headgroup) surfactants,[14] usually including low critical aggregation concentrations. Specially designed cationic gemini surfactants have recently been found to display high transfection activities.[15−17] The glucose-based gemini surfactant **1** with 9-octadecenyl chains in the natural

---

† Stratingh Institute, University of Groningen.

‡ DUBBLE CRG/ESRF.

§ Groningen Biomolecular Sciences and Biotechnology Institute, University of Groningen.

∥ Department of Organic Chemistry, University of Nijmegen.

⊥ Present address: Department of Chemistry, University College London, U.K.

(1) Anderson, W. F. *Science* **1984**, *226*, 401−409.
(2) Cavazzano-Calvo, M.; Hacein-Bey, S.; De Saint Basile, G.; Gross, F.; Yvon, E.; Nusbaum, P.; Selz, F.; Hue, C.; Certain, S.; Casanova, J.-L.; Bousso, P.; Le Deist, F.; Fischer, A. *Science* **2000**, *288*, 669−672.
(3) Lehrman, S. *Nature* **1999**, *401*, 517−518.
(4) Pearson, H. *Nature* **2000**, *413*, 9.
(5) Felgner, P. L.; Gadek, T. R.; Holm, M.; Roman, R.; Chan, H. W.; Wenz, M.; Northrop, J. P.; Ringold, G. M.; Danielsen, M. *Proc. Natl. Acad. Sci. U.S.A.* **1987**, *84*, 7413−7417.
(6) Miller, A. D. *Angew. Chem., Int. Ed.* **1998**, *37*, 1768−1785 and references therein.
(7) Barenholz, Y. *Curr. Opin. Colloid Interface Sci.* **2001**, *6*, 66−77.

(8) Mountain, A. *Trends Biotechnol.* **2000**, *18*, 119−128.
(9) Menger, F. M.; Littau, C. A. *J. Am. Chem. Soc.* **1991**, *113*, 1451−1452.
(10) Menger, F. M.; Littau, C. A. *J. Am. Chem. Soc.* **1993**, *115*, 10083−10090.
(11) Zana, R.; Bennraou, M.; Rueff, R. *Langmuir* **1991**, *7*, 1072−1075.
(12) Zana, R.; Talmon, Y. *Nature* **1993**, *362*, 228−230.
(13) Karaborni, S.; Esselink, K.; Hilbers, P. A. J.; Smit, B.; Karthauser, J.; van Os, N. M.; Zana, R. *Science* **1994**, *266*, 254−256.
(14) Menger, F. M.; Keiper, J. S. *Angew. Chem., Int. Ed.* **2000**, *39*, 1451−1452.
(15) Camilleri, P.; Kremer, A.; Edwards, A. J.; Jennings, K. H.; Jenkins, O.; Marshall, I.; McGregor, C.; Nevelle, W.; Rice, S. Q.; Smith, R. J.; Wilkinson, M. J.; Kirby, A. J. *Chem. Commun.* **2000**, 1252−1254.
(16) McGregor, C.; Perrin, C.; Kremer, A.; Camilleri, P.; Kirby, A. J. *J. Am. Chem. Soc.* **2001**, *123*, 6215−6220.
(17) Buynsters, P. J. J. A.; García Rodríguez, C. L.; Willighagen, E. L.; Sommerdijk, N. A. J. M.; Kremer, A.; Camilleri, P.; Feiters, M. C.; Nolte, R. J. M.; Zwanenburg, B. *Eur. J. Org. Chem.* **2002**, 1397−1406.
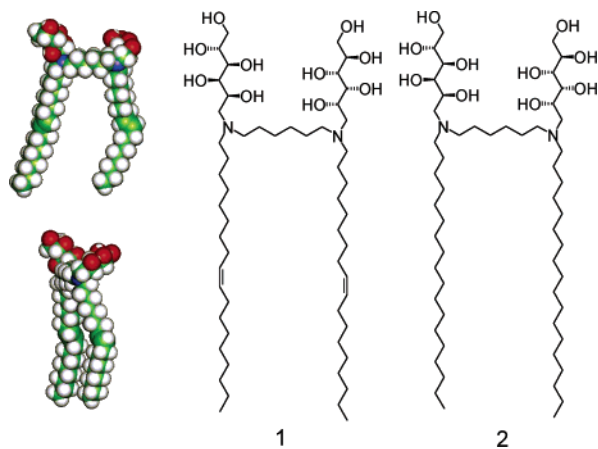
Figure 1. Chemical structure of the studied gemini surfactants. The space filling model corresponds to **1** minimized in an environment of a layer (20 Å) of water molecules using CHARMM molecular modeling software version 3.3.

Table 1. Positions of SAXS Reflections in q-Space (in Å^{-1}), Assignments (in Parentheses), and Corresponding Periodicities (Å)

sample	position in Å^{-1} (assignment)
1, vesicles	0.129 (001), $d = 48.7$ Å
1, lipoplex	
pH 8.80	0.105 (001), 0.208 (002), $d = 59.8$ Å;
	0.134 (001), $d = 46.8$ Å
pH 8.50	0.105 (001), 0.210 (002), $d = 59.8$ Å
pH 7.49	0.108 (001), $d = 58.2$ Å
pH 7.03	0.110 (001), $d = 57.1$ Å
pH 6.48	0.114 (001), 0.228 (002), $d = 55.1$ Å
pH 5.75	0.1256 (100), 0.220 (110), 0.334 (210), $a = 57.8$ Å
2, vesicles	0.138 (001), $d = 44.5$ Å
2, lipoplex	0.1205 (001), $d = 52.1$ Å

cis/trans ratio of 80%/20% and a spacer of six methylene groups (Figure 1) displays a particularly high transfection activity[18] (approximately 3 times that of the commercial transfection agent LIPOFECTAMINE 2000/+), which peaks at a surfactant to base pair ratio of 2:1 and does not require helper lipids such as DOPE (dioleoylphosphatidyl ethanolamine). Its saturated analogue **2** is less active (potency approximately one-sixth of that of **1**) and requires a much higher surfactant to base pair ratio (20:1). It has been suggested[19] that the mechanism of transfection by synthetic surfactants involves endocytosis, that is, the incorporation of foreign material by controlled invagination of the cell membrane, allowing the DNA-surfactant complex, or lipoplex, to be enveloped by the cell membrane, resulting in the budding off of a new vesicle, or endosome, inside the cell. The escape of DNA from this endosome is proposed to depend on the possibility to form a fusogenic inverted hexagonal phase.[20-23] This phase can be induced by the shape of the cationic surfactant molecule[24] or of the helper lipid,[25] or by the interaction of the lipoplex with anionic lipids.[26-28] The established effect of pH on the aggregation state of **1** and **2**[18,29] and the postulated importance of pH effects in endocytosis[30-34] prompted us to study the pH dependence of the lipoplex morphology of these compounds by SAXS (small angle X-ray scattering), cryo-TEM (cryo-transmission electron microscopy), and molecular modeling.

Results

Morphology and Packing of the Vesicles and Lipoplexes. Free Vesicles. The cryo-TEM image of **1** (Figure 2a) reveals the presence of multilamellar vesicles (diameter range 200–400 nm). The diffractograms of free vesicles of **1** and **2** (not shown) show single broad diffraction peaks at $q = 0.129$ Å^{-1} and $q = 0.138$ Å^{-1}, respectively (Table 1). Considering the well-defined lamellar structures observed in EM, we take these reflections to be the crystallographic (001) reflections of lamellar structures with spacings ($d = 2\pi/q_{001}$) of 48.7 Å (**1**) and 44.5 Å (**2**) (Table 1).

Lipoplexes at pH 8.8–8.5. The preparation of the lipoplex of **1** and salmon sperm DNA at pH 8.80 yields a turbid solution. Cryo-TEM (Figure 2b) reveals the presence of aggregates heterogeneous in both size (range 300–1000 nm) and shape, which exhibit a characteristic uneven surface, consistent with DNA molecules sandwiched between the lipid bilayers.[35-37] SAXS (Figure 3a) shows a pattern of reflections (Table 1) characteristic of a lamellar lipoplex[38] with $d = 59.8$ Å. In addition, the diffractogram showed a small peak at $q = 0.134$ Å^{-1} ($d = 46.8$ Å). This reflection falls within the range observed for DNA–DNA spacings,[39] but in view of the similarity to the spacing of the DNA-free aggregate ($d = 48.7$ Å), we prefer to ascribe it to free vesicles not complexed to DNA, which are also observed with EM (not shown). Lowering the pH to 8.50 causes an increase in the intensity and sharpness of the peaks attributed to the lamellar structure of the lipoplex (Figure 3a, Table 1), indicating that the lipoplex is the major aggregated species in solution and that the size of the domains possessing lamellar order has increased.[40] At this pH, it is reasonable to assume that the gemini surfactant molecules in the lipoplex are singly protonated. Further acidification to pH 7.97 does not lead to any change in size or spacing of the lamellar structure.

(18) Fielden, M. L.; Perrin, C.; Kremer, A.; Bergsma, M.; Stuart, M. C.; Camilleri, P.; Engberts, J. B. F. N. *Eur. J. Biochem.* **2001**, *268*, 1269–1279.
(19) Zabner, J.; Fasbender, A. J.; Moninger, T.; Poellinger, K. A.; Welsh, M. J. *J. Biol. Chem.* **1995**, *270*, 18997–19007.
(20) Ellens, H.; Siegel, D. P.; Alford, D.; Yeagle, P. L.; Boni, L.; Lis, L. J.; Quinn, P. J.; Bentz, J. *Biochemistry* **1989**, *28*, 3692–3703.
(21) Siegel, D. P.; Epand, R. M. *Biophys. J.* **1997**, *73*, 3089–3111.
(22) Audouy, S.; Hoekstra, D. *Mol. Membr. Biol.* **2001**, *18*, 129–143.
(23) Oberle, V.; Zuhorn, I.; Audouy, S.; Bakowsky, U.; Šmisterová, J.; Engberts, J. B. F. N.; Hoekstra, D. In *Targeting of Drugs*; Gregoriades, G., McCormack, B., Eds.; Plenum Press: New York, 2000; pp 146–155.
(24) Šmisterová, J.; Wagenaar, A.; Stuart, M. C. A.; Poulshkin, E.; Ten Brinke, G.; Hulst, R.; Engberts, J. B. F. N.; Hoekstra, D. *J. Biol. Chem.* **2001**, *276*, 47615–47622.
(25) Koltover, I.; Salditt, T.; Rädler, J. O.; Safinya, C. R. *Science* **1998**, *281*, 78–81.
(26) Xu, Y.; Szoka, F. C., Jr. *Biochemistry* **1996**, *35*, 5616–5623.
(27) Hafez, I. M.; Cullis, P. R. *Adv. Drug Delivery Rev.* **2001**, *47*, 139–148.
(28) Hafez, I. M.; Maurer, N.; Cullis, P. R. *Gene Ther.* **2001**, *8*, 1188–1196.
(29) Bergsma, M.; Fielden, M. L.; Engberts, J. B. F. N. *J. Colloid Interface Sci.* **2001**, *243*, 491–495.
(30) Tycko, B.; Maxfield, F. R. *Cell* **1982**, *28*, 643–651.

(31) Straubinger, R. M.; Hong, K.; Friend, D. S.; Papahadjopoulos, D. *Cell* **1983**, *32*, 1069–1079.
(32) Labat-Moleur, F.; Steffan, A.-M.; Brisson, C.; Perron, H.; Feugeas, O.; Furstenberger, P.; Oberling, F.; Brambilla, E.; Behr, J.-P. *Gene Ther.* **1996**, *3*, 1010–1017.
(33) Hafez, I. M.; Ansell, S.; Cullis, P. R. *Biophys. J.* **2000**, *79*, 1438–1446.
(34) Mellman, I.; Fuchs, R.; Helenius, A. *Annu. Rev. Biochem.* **1986**, *55*, 663–700.
(35) Lasic, D. D.; Strey, H.; Stuart, M. C. A.; Podgornik, R.; Frederik, P. M. *J. Am. Chem. Soc.* **1997**, *119*, 832–833.
(36) Mel'nikova, Y. S.; Mel'nikov, S. M.; Löfroth, J.-E. *Biophys. Chem.* **1999**, *81*, 125–141.
(37) Sternberg, B.; Sorgi, F. L.; Huang, L. *FEBS Lett.* **1994**, *356*, 361–366.
(38) Rädler, J. O.; Koltover, I.; Salditt, T.; Safinya, C. R. *Science* **1997**, *275*, 810–814.
(39) Koltover, I.; Salditt, T.; Safinya, C. R. *Biophys. J.* **1999**, *77*, 915–924.
(40) Klug, H. P.; Alexander, L. E. *X-ray Diffraction Procedures for Polycrystalline and Amorphous Materials*, 2nd ed.; Wiley-Interscience: New York, 1974; pp 687–690.
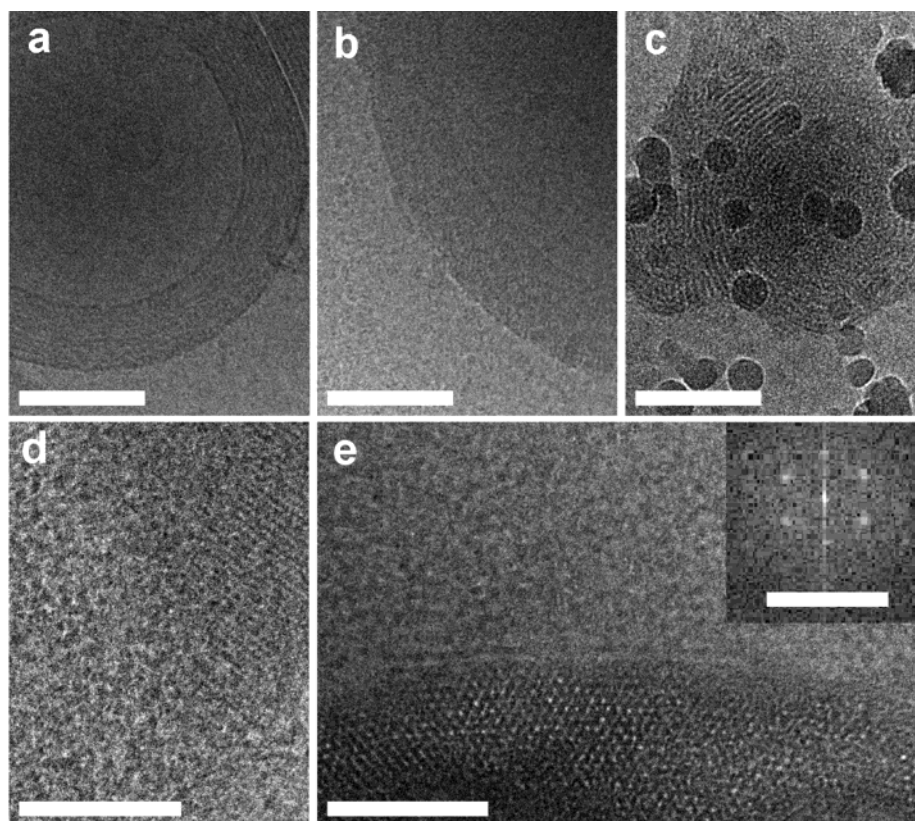
Figure 2. Cryo-electron microscopy images of **1**: (a) free (i.e., without DNA) gemini surfactant; (b) lipoplex at the pH of preparation (8.8); (c) condensed lamellar phase evident at pH 6.51 (circular structures are artifacts); (d) "side view" of hexagonal (H_{II}) phase at pH 5.13 as columns; (e) as (d) but "face on" view; inset of (e), Fourier transform pattern derived from (d). Scale bar, 100 nm, apart from the inset of (e), which is 0.5 nm^{-1}.
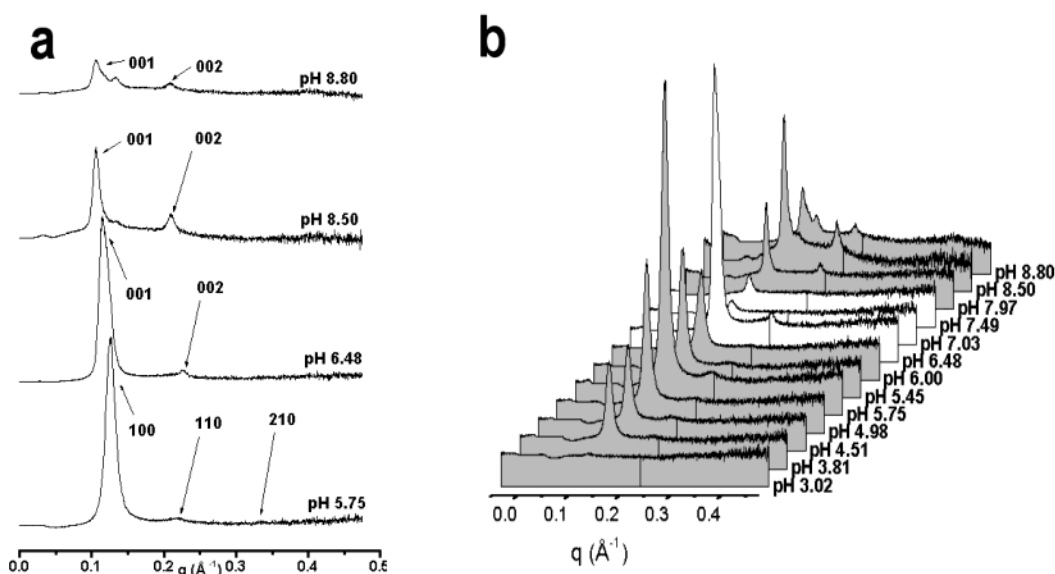

Figure 3. SAXS patterns of **1**: (a) representative diffractograms, with assignments, of the initial state of the lipoplex (pH 8.80) and the three exclusive morphologies observed, lamellar (pH 8.50), condensed lamellar (pH 6.48), and H_{II} columnar phase (pH 5.75); (b) comprehensive stack plot showing the phase transitions as a function of pH, with the phase regions in shaded plots.

Titration of Lipoplex of 1. Upon lowering the pH from pH 7.49 to pH 7.03, a transient loss of order occurs as proven by the disappearance of the (002) reflection with a decrease of the bilayer spacing to $d = 58.2$ and 57.1 Å, respectively (Figure 3b, Table 1). In this pH range, a transition to a condensed lamellar phase occurs, which is most prominent at pH 6.48 (Figure 3a) and characterized by (001) and (002) reflections (Table 1, $d = 55.1$ Å). The limited amount of acid consumed

during this transition indicates that it probably does not involve complete protonation of the second amino moiety but is driven either by increased protonation at the surface of the aggregate and a curvature-induced change or by further dehydration of the DNA. It has been previously shown[41] that the apparent pK_a

---

(41) Pector, V.; Caspers, J.; Banerjee, S.; Deriemaeker, L.; Fuks, R.; El Ouahabi, A.; Vandenbranden, M.; Finsy, R.; Ruysschaert, J.-M. *Biochim. Biophys. Acta* **1998**, *1372*, 339−346.
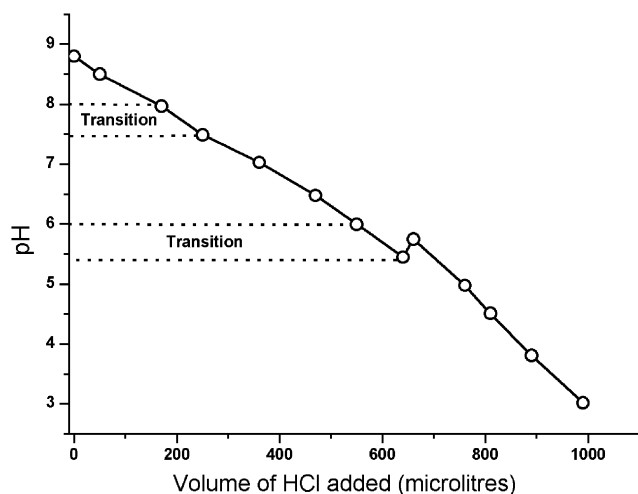
Figure 4. Graph of the volume of acid (0.1 M HCl) added to drive morphological change of the lipoplex (5 mL) of the surfactant **1** (22.8 mM) and DNA (11.35 mM in base pair). Open symbols correspond to the aliquots taken for measurements of the SAXS patterns (cf., Figure 3b).

of vesicular species is lower than the intrinsic pK_a of free amines. The approximate intrinsic pK_a values for **1** are 8.2 and 5.8,[42] whereas the approximate "vesicular" pK_a of the second amine in the lipoplex is between pH 5.5 and 4.[18,29] Cryo-TEM of the lipoplex at pH 6.51 (Figure 2c) revealed the presence of smaller complexes (100–300 nm) of more defined structure than that at pH 8.8 with the well-known spiky surface morphology.[35–37]

As can be seen in the SAXS patterns (Figure 3b), the condensed lamellar lipoplex undergoes a further transition between pH 6.00 and 5.45 to an inverted hexagonal columnar phase. Interestingly, the largest ordered domains, with a characteristic set of (100), (110), and (210) reflections (Figure 3a, Table 1) and a cell spacing ($a = 4\pi/[(3)^{0.5}q_{100}]$) of 57.8 Å, are observed upon the addition of more acid at pH 5.45, showing, surprisingly, an initial *increase* in the pH of the solution to 5.75 (Figure 4). A (200) reflection is typically also observed in such systems[25] but is not observed in our system, possibly because the value of the form factor (see Appendix) happens to be very low at the position where it is expected. This may be related to a distortion from the ideal hexagonal lattice or, as accounted for in detail in the Appendix, may be explained by effects of varying electron density in the cylinders, as the aromatic moieties and phosphate groups of the DNA are expected to have a higher electron density than the surrounding lipid. Cryo-TEM confirms the presence, at pH 5.13, of a lipoplex with a hexagonal (H$_{II}$) morphology, shown in Figure 2d and e in different orientations, highlighting the columnar character-istics and the hexagonal order, respectively. The Fourier transform of this image (Figure 2e, inset) clearly shows the packing of the aggregate with an observed *a* spacing of approximately 56 Å, which compares well with the SAXS-derived value. According to the SAXS data, the well-defined order of this hexagonal phase is destroyed upon further acidification of the solution to pH 3. At this low pH, micelles are formed,[18] and no defined order could be observed (Figure 3b).

Comparison with 2. In contrast to the rich variety in packing modes displayed by the lipoplex of **1**, there was no evidence

for any structural variations in the lipoplex of **2** upon a change in pH. A broad reflection at $q = 0.1205$ Å^{-1} ($d = 52.1$ Å) was found at high pH and remained constant in both position and intensity throughout the pH range 8.8–3.0 with no evidence for a (002) reflection (not shown). The difference in behavior of the compounds highlights that the double bond present in the tails of **1**, but not in **2**, is an essential structural element in facilitating the morphological changes in the lipoplex and allowing the concomitant variation in tail packing upon changing the pH. This difference is also reflected in the gel to liquid-crystal phase transition temperature (T_c) of the DNA-free bilayer, which is 55 °C for **2** but below 0 °C for **1**.[18] The higher flexibility of the alkyl tails of **1** accounts for the relatively large increase in lamellar spacing (11.1 Å) upon DNA complexation as compared to only 7.6 Å for **2**, and its much larger pH sensitivity. Clearly, the unsaturated 9-octadecenyl tails in **1** reduce the resistance of the bilayers to morphological changes upon DNA complexation and pH variation. The lower value for the lamellar spacing of **2** as compared to **1** in the lipoplex at high pH ($d = 52.1$, respectively, 59.8 Å, cf. Table 1) indicates that the saturated alkyl tails in **2** are more strongly interdigitated than the unsaturated alkyl tails in **1** (see also the Molecular Modeling section). The lipoplex formed with **2** is most likely inappropriately condensed, resulting in less efficient transfection. This conclusion is in line with the results of recent studies in which derivatives of the pyridinium amphiphiles (so-called SAINTs) with saturated and unsaturated tails are compared.[43]

Molecular Modeling. To visualize the postulate that the DNA is templating a morphological change at a critical pH, we performed modeling studies on energy-minimized **1** (Figure 1) and a standard B-DNA double helix, using packings and geometrical information derived from SAXS and EM as boundary conditions. The spacing of the bilayers in the free vesicles is obtained with intercalation of the alkyl tails up to the double bonds (Figure 5, top left). Bilayer formation with intercalation is also observed in a recent Molecular Dynamics study of the analogue with hexadecyl tails instead of the 9-octadecenyl and octadecyl chains in, respectively, **1** and **2**,[44] and is in line with SAXS results for that compound.[18] The lamellar phase for the lipoplex of **1** is illustrated (Figure 5, middle) for DNA possessing a 20 Å diameter and the alkyl chains intercalating to the double bond to reproduce the measured 59.8 Å spacing. The observed complementarity of the spacing between the phosphate groups spacing across the minor groove in the DNA (10 Å) to the ammonium function-alities of the doubly charged gemini surfactant (9.5 Å) is almost perfect (Figure 5, bottom). This indicates that cationic gemini surfactants require a spacer of six methylene groups for optimum transfection efficiency. (However, other factors will also play a role, and conclusions regarding the optimum spacer length should be treated with caution as **2** does not show more transfection activity than its analogue with a spacer of only four methylene groups.[18]) Finally, the possibility of the sugar headgroups of **1** to sit in the major grooves of DNA in the lipoplex structure prevents these functionalities from hindering "localized" surfactant ammonium/DNA phosphate interactions (Figure 5, top right).

(42) Johnsson, M.; Engberts, J. B. F. N. *J. Am. Chem. Soc.*, in press.

(43) Zuhorn, I. S.; Oberle, V.; Visser, W. H.; Engberts, J. B. F. N.; Bakowsky, U.; Polushkin, E.; Hoekstra, D. *Biophys. J.* **2002**, *83*, 2096–2108.

(44) Van Eijk, M. C. P.; Bergsma, M.; Marrink, S.-J. *Eur. Phys. J. E* **2002**, *7*, 317–324.
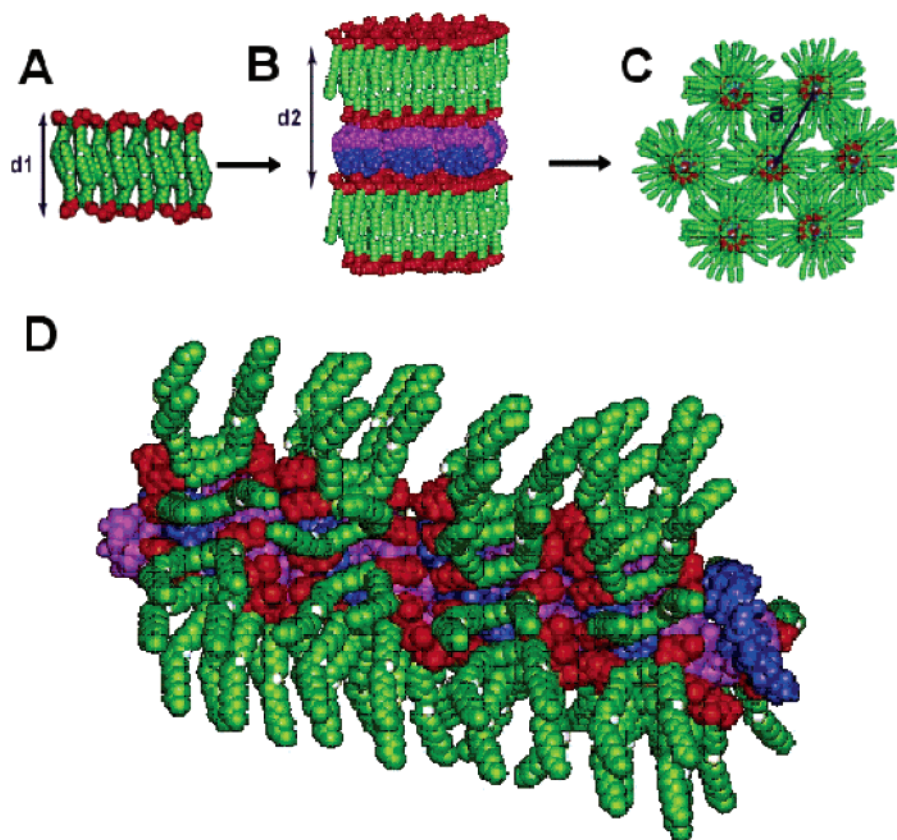
Figure 5. Space filling molecular models of aggregates of **1** and DNA based on SAXS/EM derived morphology and geometry: (a) free vesicles, $d1 = 48.7$ Å; (b) initial lamellar phase of lipoplex, $d2 = 59.8$ Å; (c) columnar H_{II} structure of lipoplex, $a = 57.8$ Å; (d) model depicting complementary arrangement of the gemini surfactant amino groups (9.5 Å spacing) with the DNA phosphate groups across the minor groove (10 Å spacing). Color code: green, alkyl tails; red, sugar headgroups; blue and purple, complementary DNA strands.

Discussion

We assert that the acid-induced change in morphology of the lipoplex formed from **1** and salmon sperm DNA from condensed lamellar to inverted hexagonal must be driven by a close association of largely doubly protonated surfactant molecules with the DNA phosphate groups. The increase in pH that accompanies this event (cf. Figure 4) is due to the concomitant exposition and protonation of unprotonated amine functionalities that were initially internalized in the condensed bilayers. In earlier studies on these gemini surfactants,[18,29] a proton-induced vesicle-to-micelle transition was observed and explained by significant protonation of the second amine moiety. This would cause a larger degree of counterion association and increased hydration, leading to an increase in the headgroup size, which favors micelles over bilayers in line with the shape-structure concept.[45] The change from a lamellar to an inverted hexagonal phase observed here for the lipoplex of **1** requires a decrease in headgroup size and can be rationalized by a strong association between the doubly charged headgroup of **1** and phosphate moieties of the DNA, leading to (i) local charge neutralization and (ii) dehydration of both the phosphate groups and the headgroups, which result in an effective reduction in headgroup size. The occurrence of the morphological change at pH 5.45 is consistent with a vesicular pK_a for **1** around this pH value. Thus, we postulate that DNA is a *template* for the H_{II} columnar phase due to "specific" association of pairs of phosphates with the doubly charged gemini, as opposed to the "atmospheric" (i.e., weakly localized, dynamic) DNA association with the singly charged species observed in the lamellar phases. The lipoplex of **2**, the saturated analogue of **1**, does not undergo pH-induced morphological changes.

The pH-induced formation of an inverted hexagonal (H_{II}) phase for the lipoplex of **1** and DNA in the endosomal pH range, as evidenced by our SAXS and cryo-SEM results, facilitates its fusion with the endosomal membrane, an important step toward release of the DNA into the cytoplasm.[20–28] An additional factor that could possibly contribute to the escape of the DNA from the endosome is the increase in osmotic pressure caused by the anomalous pH increase observed in our system upon acidification at pH 5.45.

The observation of the pH-induced and DNA-templated formation of the hexagonal phase of the lipoplex allows us to propose a detailed mechanism for the transfection by **1** as presented in Figure 6. Passage of the membrane by endocytosis was demonstrated by Zabner et al.,[19] using electron microscopy for the lipoplex of gold-labeled DNA and a 1:1 mixture of DMRIE (*N*-[1-(2,3-dimyristyloxy)propyl]-*N*,*N*-dimethyl-*N*-(2-hydroxyethyl)ammonium bromide) and DOPE. A stepwise mechanism for transfection with cationic lipids by endocytosis followed by release through destabilization of the endosomal membrane, due to the interaction of cationic and anionic lipids, was first proposed by Xu and Szoka.[26] Bhattacharya and Mandal[46] have shown that anionic surfactants can liberate DNA

(45) Israelachvili, J. N.; Marčelja, S.; Horn, R. G. *Q. Rev. Biophys.* **1980**, *13*, 121–200.

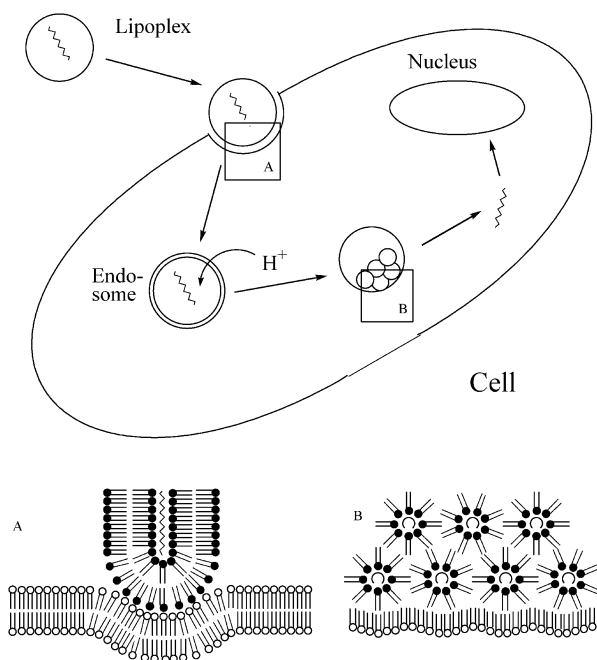(46) Bhattacharya, S.; Mandal, S. S. *Biochemistry* **1998**, *37*, 7764–7777.

Figure 6. Proposed mechanism, adapted from Xu and Szoka (ref 26), for transfection mediated by **1** involving the formation of a pH-induced DNA-templated fusogenic hexagonal phase which allows escape from the endosome. Zwitterionic/anionic membrane components and cationic gemini surfactants are schematically represented with white and black headgroups, respectively. Insets A and B are detailed representations of the areas in the labeled boxes: A, onset of endocytosis of the lipoplex at the cell membrane; B, formation of the fusogenic DNA-templated hexagonal phase in the endosome at low pH.

from lipoplexes with cationic lipids. The model was refined in detail by Cullis and co-workers,[28] who established by ^{31}P NMR that the interaction of a lipoplex with aggregates of anionic phospholipids, viz., of a lipoplex of plasmid DNA-DOTAP (*N*-(2,3)-dioleyloxypropyl)-*N,N,N*-trimethylammonium methyl sulfate) complex with large unilamellar DOPS (dioleoylphosphatidylserine) vesicles, results in formation of an inverted hexagonal phase. Although it is of importance for the mechanism of transfection that such a fundamental change in morphology of the lipoplex can occur just by an encounter with anionic membranes, the question arises why it does not occur immediately when the lipoplex interacts with either the cell or the endosomal membrane (situations A and B in Figure 6, respectively). A possible explanation could be the asymmetry in distribution of anionic lipids over the inner and outer leaflets of the membrane.[47] Because it has been shown by electron microscopy[19] that the DNA is found in endosomes but not in lysosomes, we propose that the factor that triggers the escape of the DNA from the endosome is the gradual decrease in pH[30] that this organelle undergoes after formation. Our finding that the inverted hexagonal phase can be formed with cationic lipids alone, upon lowering the pH, is important for the mechanism of transfection because it provides a reasonable explanation of why escape occurs from the endosome under these circumstances.

Conclusion

The potential of **1** to form a lamellar lipoplex which changes to the fusogenic inverted hexagonal phase at a critical (endo-

(47) Gennis, R. B. *Biomembranes: Molecular Structure and Function*; Springer-Verlag: New York, 1989; pp 20−35.

somal) pH is proposed to be a dominant reason for its exceptional efficacy in gene transfection. This ability is derived from its specific structural features: (a) an alkyl spacer of six carbons between the amino moieties in the surfactant, which enables the ideal spacing of the ammonium groups to complement the DNA phosphate groups on either side of the minor groove, allowing DNA to template the morphology of the complex into the fusogenic inverted H_{II} columnar phase; (b) two amine nitrogen atoms in the headgroup which can be protonated, with the second amine possessing a vesicular pK_a that is in the endosomal pH region, thus causing a morphological change at a critical pH; (c) unsaturated alkyl chains which reduce T_c to below physiological temperatures and thereby increase the susceptibility of the aggregate to morphological change; and (d) hydrophilic sugar headgroups that increase the aqueous solubility but do not obstruct localized ammonium−phosphate interactions. The application of these insights as structural guidelines to surfactant and polymer design highlights the necessity to concentrate attention not just on molecular methods of DNA release from a lipoplex (e.g., surfactants with chemically labile moieties), but also on the supramolecular aggregate-driven processes which can be engineered to take place upon changes in critical cellular conditions such as pH.

Experimental Section

Materials. Compounds **1** and **2** were prepared as described earlier.[18,48] The DNA used in this study was salmon sperm DNA (ACROS, 300−1000 bp).

Sample Preparation. The lipoplexes were formed at a 2:1 surfactant/DNA base pair ratio (the most effective formulation for transfection efficiency) and at concentrations of 27.5 mM and 11 mM of surfactants **1** and **2**, respectively (limits of solubility). The pH was reduced by sequential addition of 0.1 M HCl in 5−10 μL aliquots and was continuously monitored (Figure 4). Vesicular solutions were prepared by addition of solid surfactant to double distilled water with sonication and heating to 45 °C. Sometimes the properties of a vesicle dispersion may slightly depend on the exact procedure for the vesicle preparation. In particular, small differences in size distribution can occur. In our study, we did not observe a significant difference in the case of vesicle preparation by sonication or sonication followed by extrusion.[18] Lipoplexes were prepared by the addition of a 66 mM (charge concentration) solution of DNA to the vesicular solutions. Solutions were prepared in 5 mL volumes, and aliquots of 60−100 μL were removed for the SAXS study after each acidification step.

Cryo-TEM. Samples were prepared by vitrification in liquid ethane. The grids were then transferred to a Gatan model 626 cryo-EM holder and examined under low-dose conditions at −170 °C in a CM120 Philips microscope operating at 120 keV.

SAXS. SAXS experiments were performed on the SAXS station at the Dutch-Flemish beamline (DUBBLE), BM 26, at the European Synchrotron Radiation Facility in Grenoble, France.[49] SAXS data have been recorded with the gas multiwire one-dimensional detector at a sample to detector distance of 1.5 m, with an X-ray wavelength of 1.24 Å. The SAXS data were successively normalized for absorption and detector uniformity. Background scattering due to the solvent was subtracted. The diffraction patterns are represented as $I(q) \times q^2$ to highlight details at higher q values. Spatial calibration was performed with silver behenate[50] with an estimated error margin of ±0.5% in the observed periodicities.

(48) Pestman, J. M.; Terpstra, K. R.; Stuart, M. C. A.; Van Doren, H. A.; Brisson, A.; Kellogg, R. M.; Engberts, J. B. F. N. *Langmuir* **1997**, *13*, 6857−6860.
(49) Bras, W. *J. Macromol. Sci., Phys. B* **1998**, *37*, 557−565.
(50) Blanton, T. N.; Huang, T. C.; Toraya, H.; Hubbard, C. R.; Robie, S. B.; Louer, D.; Goebel, H. E.; Will, G.; Raftery, T. *Powder Diffr.* **1995**, *10*, 91−100.

Molecular Modeling. Graphical representations of the surfactant aggregates and lipoplexes were generated on a Silicon Graphics Workstation using QUANTA/Charmm software. The initial surfactant structure was minimized in an environment with a layer (20 Å) of water molecules using CHARMM molecular modeling software version 3.3. A 50 base pair double strand B-DNA structure was constructed of a random AT sequence using the Quanta package. The proposed lipoplex geometries shown are van der Waals space filling graphical representations of the various aggregates and match the periodicities derived from the SAXS experiment.

Appendix

Calculations of the effect of cylindrical packing and variation in electron density on the form factor of the lipoplex, accounting for a variation of intensity in the SAXS reflections, follow.

Consider the scattered intensity

$$I(q) \cong N \cdot F^2(q) \cdot S(q) \qquad (1)$$

where F represents the form factor, S represents the structure factor, and N represents the number of particles in an irradiated volume. The form factor F is determined by

$$F = *(\rho_{elec}) \qquad (2)$$

where $*(\rho_{elec})$ represents the Fourier transform of the electron density distribution.

The scattering by the lipoplex can be considered as a planar problem with cylindrical symmetry. As the system is essentially scalar, that is, there is no preferred orientation in the sample, q is scalar.

Two cases should be considered.

(1) Rods of radius r_0 with uniform electron density distribution:

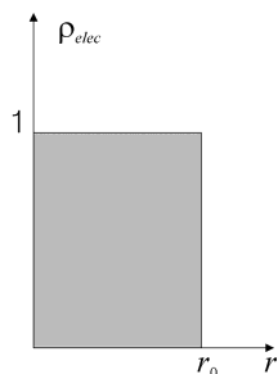One may model the electron density distribution by a boxlike function (Figure 7).

Figure 7. Model of rods of radius r_0 with uniform electron density distribution.

It can be shown that in this case the electron density and

form factor can be defined as[51]

$$\rho_{elec}(r) = \int_0^\infty F(q) \cdot J_0(qr) \cdot q \, dq \qquad (3)$$

$$F(q) = 2\pi \int_0^\infty \left(\frac{d\rho_{elec}}{dr}\right)(r) \cdot \frac{J_1(qr)}{q} \cdot r \, dr \qquad (4)$$

where J_0 and J_1 are the Bessel functions of the zero- and first-order, respectively.

For the density distribution function shown above, one ends up with

$$F(q) = 2\pi \cdot r_0{}^2 \frac{J_1(qr_0)}{qr_0} \qquad (5)$$

The first minimum occurs at $qr_0 = 3.84$.

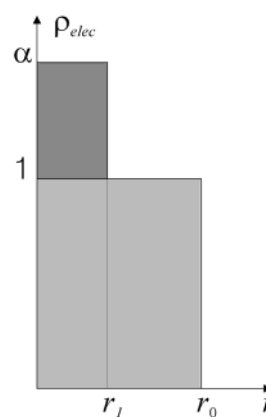(2) Core−shell rods with two different densities (Figure 8):

Figure 8. Model of core−shell rods with two different densities.

In this situation, the form factor can be deduced as follows

$$F(q) = 2\pi \cdot r_0 \frac{J_1(qr_0)}{q} + 2\pi \cdot \alpha \cdot r_1 \frac{J_1(qr_1)}{q} \qquad (6)$$

This is most likely to be the case for the lipoplex of **1**. The electron density of the DNA is apparently higher than that of
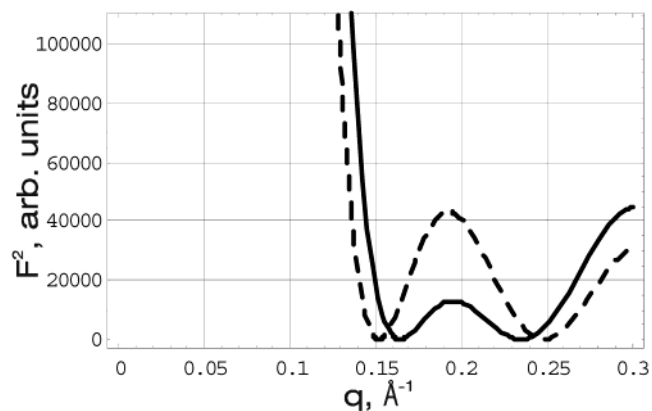

Figure 9. Scattering curve as determined by form factor for case (2) with $2r_0 = 54$ Å. Solid line, $\alpha = 1$; dashed, $\alpha = 0.5$.

the surrounding lipids due to phosphate and aromatic nucleotide groups of the DNA. As an example, if one takes $\alpha = 0.5-1$,

(51) Vainshtein, B. K. *Diffraction of X-ray by Chain Molecules*; Elsevier: Amsterdam, 1966.

the DNA diameter as 20 Å ($=2r_1$), and a diameter for the DNA$-$lipids cylinder of $52-54$ Å ($=2r_0$), one obtains the scattering curve as shown in Figure 9.

A deep minimum develops around $q = 0.25$ Å^{-1}. The pattern can be in fact smeared to some extent by the possible size polydispersity of the lipoplexes, so that I is not necessarily equal to 0 at the minimum, but at any rate, its value can be quite low.

Note Added after ASAP: The version of this paper published 1/17/2003 on the Web did not include the axes labels for Figure 9. The final Web version published 1/23/2003 and the print version are correct.

JA020707G